SAN096-1738C
CONF-9606110--4

Implant Activation and Redistribution of Dopants in GaN

J. C. Zolper,[a] S. J. Pearton,[b] R. G. Wilson,[c] and R. A. Stall[d]

[a]Sandia National Laboratories, Albuquerque, NM, 87185-0603
[b]S. J. Pearton, Un. of Florida, Gainesville, FL, 32611
[c]R. G. Wilson, Hughes Research Laboratories, Malibu, CA, 90265
[d]R. A. Stall, Emcore Corp., Somerset, NJ, 08873

Abstract- GaN and related III-Nitride materials (AlN, InN) have recently been the focus of extensive research for photonic and electronic device applications. As this material system matures, ion implantation doping and isolation is expected to play an important role in advance device demonstrations. To this end, we report the demonstration of implanted p-type doping with Mg+P and Ca as well as n-type doping with Si in GaN. These implanted dopants require annealing ~1100 °C to achieve electrical activity, but demonstrate limited redistribution at this temperature. The redistribution of other potential dopants in GaN (such as Be, Zn, and Cd) will also be reported. Results for a GaN junction field effect transistor (JFET), the first GaN device to use implantation doping, will also be presented.

I. INTRODUCTION

The III-Nitride material system has been the focus of extensive research for application to uv emitters and detectors [1,2]. In addition, this material system is attractive for use in high-temperature or high-power electronic devices [3,4]. A primary reason for the recent advances in III-N based photonic devices was the demonstration of p-type doping of GaN during MOCVD growth followed by a dehydrogenation anneal to activate the Mg acceptors [5,6]. Moreover, since ion implantation has been the foundation of most advanced electronic and, to a lesser extent, photonic devices in mature semiconductor materials systems such as silicon and gallium arsenide[7] it is important to determine the applicability of ion implantation to III-N based devices. In particular the demonstration of selective area implant isolation and doping will allow new III-N based device structures such as lasers and FETs with selectively doped contact regions, planar waveguides created by implant isolation, and implantation tailored current guiding in LEDs and lasers, to name a few. In this paper, we present results for the successful n- and p-type implant doping of GaN that lead to the first GaN junction field effect transistor (JFET). The JFET was produced with all ion implantation doping.

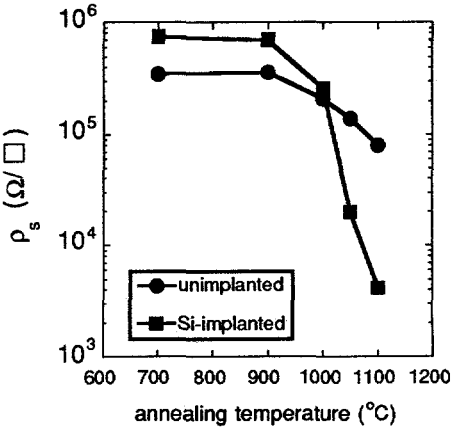

Fig 1. Sheet resistance versus annealing temperature for Si-implant (200 keV, $5e10^{14}$ cm^{-2}) and unimplanted GaN.

II. N- AND P-TYPE IMPLANT DOPING

Figure 1 shows the evolution of sheet resistance versus annealing temperature for Si-implanted (200 keV, $5x10^{14}$ cm^{-2}) and unimplanted GaN [8]. The samples were annealed for 10 s in flowing N_2 in a SiC coated graphite susceptor. It is critical to use a hydrogen free ambient to avoid hydrogen passivation of the dopants and thus to achieve electrical activity. As seen in Fig. 1, electrical activity starts to occur at 1050 °C, as evident by the drop in sheet resistance, and further increases at 1100 °C.

Figure 2 shows the evolution of sheet resistance versus annealing temperature for Mg (180 keV, $5x10^{14}$ cm^{-2}), Mg+P (180/250 keV, both $5x10^{14}$ cm^{-2}), and unimplanted GaN. The Mg-only samples remain n-type up to 1100 °C

DISCLAIMER

while the Mg samples co-implanted with P convert from n-to-p type after a 1050 °C anneal. The effect of the P co-implantation may be explained by a reduction of N-vacancies or an increase in Ga-vacancies leading to a higher probability of Mg occupying a Ga-site. Co-implantation of P has also been shown to be effective in enhancing activation and reducing diffusion for p-type implantation in GaAs [9] The ionization levels of implanted Mg has also been determined from an Arrhenius plot of carrier density to be 171 meV and is consistent with the value reported for epitaxial Mg-doped GaN [10,1].

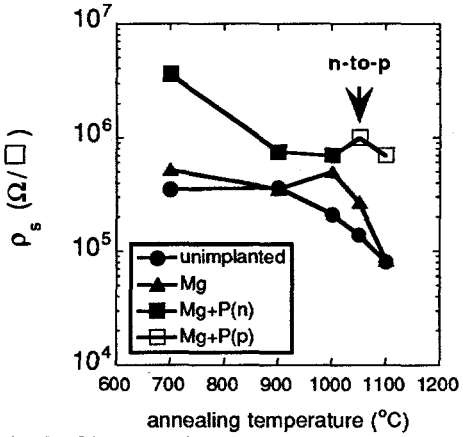

Fig 2. Sheet resistance versus annealing temperature for Mg-implanted (180 keV, $5e10^{14}$ cm^{-2}), Mg+P (180/250 keV, $5e10^{14}$ cm^{-2}) implanted, and unimplanted GaN.

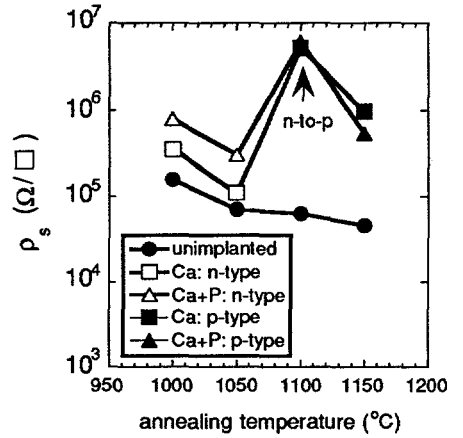

Fig 3. Sheet resistance versus annealing temperature for Ca-implanted (180 keV, $5e10^{14}$ cm^{-2}), Ca+P (180/130 keV, $5e10^{14}$ cm^{-2}) implanted, and unimplanted GaN.

Since the ionization level of Mg in GaN is much greater than kT, less than 1% of the Mg-acceptors will be ionized at room temperature. Therefore, it would be desirable to identify an acceptor species with a smaller ionization energy. Since Ca has been suggested theoretically to be a shallow acceptor in GaN [11]; ion implantation was used to determine the ionization energy of Ca in GaN [12]. Figure 3 shows the evolution of sheet resistance versus annealing temperature of Ca (180 keV, $5x10^{14}$ cm^{-2}), Ca+P (180/130 keV, both $5x10^{14}$ cm^{-2}), and unimplanted GaN. Both the Ca-only and the Ca+P samples convert from n-to-p type after a 1100 °C anneal with a further increase in p-type conduction after a 1150 °C anneal. The fact that P co-implantation is not required to achieve p-type conductivity with Ca can be understood based on the higher mass of the Ca-ion, as compared to Mg, generating more implantation damage and therefore more Ga-vacancies. This explanation is supported by the higher activation temperature required for conversion from n-to-p type for the Ca-implanted samples compared to the Mg+P implanted samples. The ionization level of Ca was estimated from an Arrhenius plot to be 169 meV [12], which is equivalent to that of Mg. Although the ionization level of Ca is not less than that of Mg, Ca may be preferred for forming shallow implanted p-regions in GaN due to its heavier mass and resulting smaller projected range and straggle than Mg for a given energy.

III. IMPURITY REDISTRIBUTION

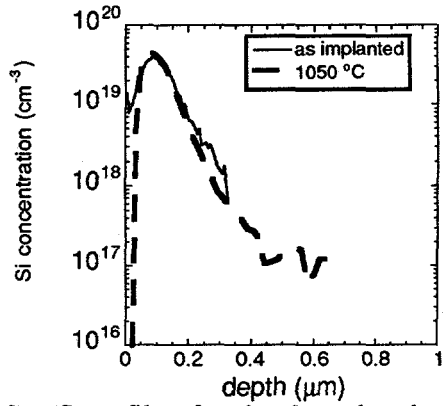

Fig 4. SIMS profile of as implanted and annealed (1050 °C, 15 s) Si (100 keV, $5x10^{14}$ cm^{-2}) in GaN.

A. Donor Species

When applying ion implantation doping to device structures it is important to know how the impurities redistribute during the activation anneal. Initial studies on the redistribution of implanted impurities in GaN were limited to temperatures up to ~800 °C [13]. However, when it became apparent that temperatures on-the-order-of 1100 °C are required to achieve activated dopants the

question of redistribution was revisited [14]. Figure 4 shows the Secondary Ion Mass Spectroscopy (SIMS) profile for ^{28}Si in GaN as-implanted and annealed (1050 °C). Despite the interference in the mass 28 SIMS signal from $^{28}N_2$, the annealed Si profile demonstrates no measurable redistribution. Using a conservative estimate of 20 nm for the resolution of the SIMS measurement, an upper limit of 2.7×10^{-13} cm/s can be set on the diffusivity of Si in GaN at 1050 °C.

B. Acceptor Species

The lack of Si-redistribution at the implant activation temperature is consistent with the behavior of Si in other compound semiconductors; however, acceptor species are generally more susceptible to diffusion at high temperatures. Figure 5 shows the SIMS profiles for Mg, as-implanted and after a 1150 °C, 15 s anneal. After annealing the Mg-profile shows a slight movement towards the surface that is estimated to be 50 nm near the peak of the profile. Based on a 50 nm diffusion length and a 15 s anneal, an upper limited of 6.7×10^{-13} cm/s can be set on the diffusivity of Mg in GaN at 1150 °C. Profiles for Mg co-implanted with P demonstrated a similar amount of redistribution that is somewhat in contrast to the need for co-implantation to achieve acceptor activity since the Mg-only sample should have more Mg in non-active, interstitial sites that should act as fast diffusers as they do in other compound semiconductors. This potential conflict has not yet been resolved.

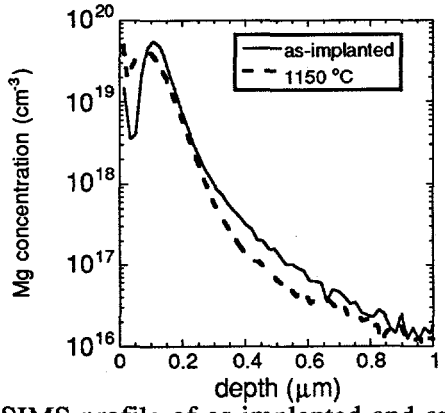

Fig 5. SIMS profile of as implanted and annealed (1150 °C, 15 s) Mg (200 keV, 5×10^{14} cm^{-2}) in GaN.

Finally, as shown in Fig. 6, implanted Ca also shows no measurable redistribution even at 1125 °C [12]. The lack of significant redistribution of all the acceptor and donor species studied suggests that ion implantation will be a viable technology for controllable doping of GaN. Furthermore, due to the lack of diffusion, external source diffusion appears not to be practical in GaN.

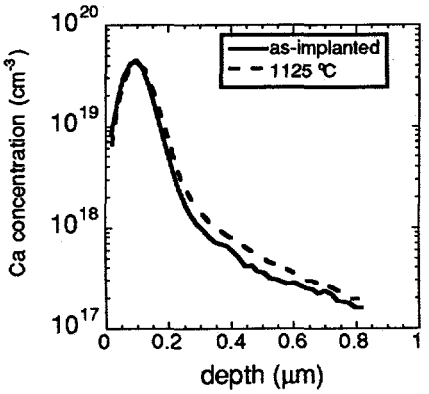

Fig 6. SIMS profile of as implanted and annealed (1125 °C, 15 s) Ca (180 keV, 5×10^{14} cm^{-2}) in GaN.

IV. GaN JFET

As discussed earlier, ion implantation doping and isolation has played a critical role in the realization of many high performance devices in most mature semiconductor materials systems such as Si and GaAs. This is also expected to be the case for III-N based devices as the quality of the III-N materials continues to improve. Even though the III-N materials are far from mature, all ion implanted transistors have already been demonstrated [15].

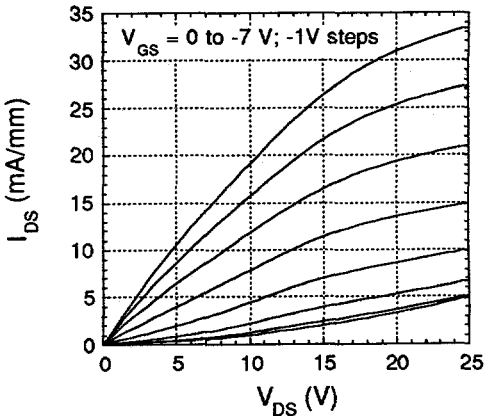

Fig 7. I_{DS} versus V_{DS} for varied V_{GS} for a 0.7x50 μm^2 all ion implanted GaN JFET.

Figure 7 shows the I_{DS} versus V_{DS} curves for varied gate biases for a ~1.7 μm x 50 μm GaN JFET with a 4 μm source-to-drain spacing fabricated with all implanted dopants. The JFET

demonstrates good modulation characteristics with nearly complete pinch-off at a threshold voltage of approximately -6 V for V_{DS} = ~7V. For V_{DS} = 25 V, a maximum transconductance of 7 mS/mm was measured at V_{GS} = -2.0 V with a saturation current of 33 mA/mm at V_{GS} = 0 V. These devices had a unity current gain cutoff frequency (f_t) of 2.7 GHz and a maximum oscillation frequency (f_{max}) of 9.4 GHz at V_{GS} = 0 V and V_{DS} = 25 V. These frequency metrics are in the range reported for epitaxial GaN MESFETs [16].

V. CONCLUSION

As with other semiconductor material systems, ion implantation is expected to play an enabling role for advanced device fabrication in the III-Nitride material system. As reported here, ion implantation has already been used to achieve n- and p-type doping of GaN and to fabricate the first GaN JFET. As further understanding is obtained on implantation induced defects, activation annealing, and the role of other impurities in these materials, it is anticipated that ion implantation will be more widely used for III-Nitride devices.

VI. ACKNOWLEDGMENT

The work performed at Sandia was supported by the DOE under contract #DE-AC04-94AL85000. The work at UF is partially supported by a National Science Foundation grant (DMR-9421109) and a University Research Initiative grant from ONR (N00014-92-5-1895). The work at Hughes was supported by ARO (Dr. J. M. Zavada). The work at EMCORE was supported by BMDO-IST managed by M. Yoder at ONR. This work was further supported by a DARPA grant (A. Husain) administered by AFOSR (G. L. Witt).

VII. REFERENCES

[1] I. Akasaki, H. Amano, M. Kito, and K. Hiramatsu, J. Lumin. **48/49** 666 (1991).

[2] S. Nakamura, T. Mukai, and M. Senoh, Appl. Phys. Lett. **64**, 1687 (1994).

[3] M. A. Khan, A. Bhattarai, J. N. Kuznia, and D. T. Olson, Appl. Phys. Lett. **63**, 1214 (1993).

[4] S. C. Binari, L. B. Rowland, W. Kruppa, G. Kelner, K. Doverspike, and D. K. Gaskill, Elect. Lett. **30**, 1248 (1994).

[5] H. Amano, M. Kito, K. Hiramatsu, and I. Akasaki, Jap. J. Appl. Phys. **28** L2112 (1989).

[6] S. Nakamura, T. Mukai, M. Senoh, and N. Iwasa, Jap. J. Appl. Phys. **31** L139 (1992).

[7] see for example: J. F. Ziegler, ed., Handbook of Ion Implantation Technology (Elsevier Science Publishers, The Netherlands, 1992) pp. 271-362; S. K. Ghandi, VSLI Fabrication Principles: Silicon and Gallium Arsenide (John Wiley & Sons, New York, 1982) chapter 6.

[8] S. J. Pearton, C. R. Abernathy, C. B. Vartuli, J. C. Zolper, C. Yuan, R. A. Stall, Appl. Phys. Lett. **67**, 1435 (1995).

[9] M. E. Sherwin, J. C. Zolper, A. G. Baca, T. J. Drummond, R. J. Shul, A. J. Howard, D. J. Rieger, R. P Schneider, and J. F. Klem, J. Elec. Mater. **15**, 809 (1994).

[10] J. C. Zolper, M. Hagerott Crawford, S. J. Pearton, C. R. Abernathy, C. B. Vartuli, C. Yuan, and R. A. Stall, J. Electron. Mat. **25**, 839 (1996).

[11] S. Strite, Jpn. J. Appl. Phys. **33**, L699 (1994).

[12] J. C. Zolper, R. G. Wilson, S. J. Pearton, and R. A. Stall, Appl. Phys. Lett. **68**, 1945 (1996).

[13] R. G. Wilson, S. J. Pearton, C. R. Abernathy, and J. M. Zavada, Appl. Phys. Lett. **66**, 2238 (1995).

[14] J. C. Zolper, M. Hagerott Crawford, S. J. Pearton, C. R. Abernathy, C. B. Vartuli, J. Ramer, S. D. Hersee, C. Yuan, and R. A. Stall, Conf. Proc. MRS, Fall 1995, symposium AAA (Material Research Society, Pittsburgh PA, in press).

[15] J. C. Zolper, R. J. Shul, A. G. Baca, R. G. Wilson, S. J. Pearton, and R. A. Stall, Appl. Phys. Lett. **68**, 2273 (1996).

[16] S. C. Binari, Proc. Sym. on Wide Bandgap Semiconductors and Devices, Fall ECS meeting 1995 (The Electrochemical Society, Pennington, NJ, 1995) p. 136.